HHS Public Access

Author manuscript

Biomaterials. Author manuscript; available in PMC 2018 February 01.

Published in final edited form as:

Biomaterials. 2017 February ; 117: 1–9. doi:10.1016/j.biomaterials.2016.11.039.

Mutant CCL2 Protein Coating Mitigates Wear Particle-Induced Bone Loss in a Murine Continuous Polyethylene Infusion Model

Akira Nabeshima[1], **Jukka Pajarinen**[1], **Tzu-hua Lin**[1], **Xinyi Jiang**[1], **Emmanuel Gibon**[1], **Luis A. Córdova**[1,3], **Florence Loi**[1], **Laura Lu**[1], **Eemeli Jämsen**[1], **Kensuke Egashira**[4], **Fan Yang**[1,2], **Zhenyu Yao**[1], and **Stuart B Goodman**[1,2,*]

[1]Department of Orthopaedic Surgery, Stanford University, Stanford, CA

[2]Department of Bioengineering, Stanford University, Stanford, CA

[3]Department of Oral and Maxillofacial Surgery, Faculty of Dentistry, University of Chile, Santiago, Chile

[4]Department of Cardiovascular Research, Development, and Translational Medicine, Kyushu University, Fukuoka, Japan

Abstract

Wear particle-induced osteolysis limits the long-term survivorship of total joint replacement (TJR). Monocyte/macrophages are the key cells of this adverse reaction. Monocyte Chemoattractant Protein-1 (MCP-1/CCL2) is the most important chemokine regulating trafficking of monocyte/macrophages in particle-induced inflammation. 7ND recombinant protein is a mutant of CCL2 that inhibits CCL2 signaling. We have recently developed a layer-by-layer (LBL) coating platform on implant surfaces that can release biologically active 7ND. In this study, we investigated the effect of 7ND on wear particle-induced bone loss using the murine continuous polyethylene (PE) particle infusion model with 7ND coating of a titanium rod as a local drug delivery device. PE particles were infused into hollow titanium rods with or without 7ND coating implanted in the distal femur for 4 weeks. Specific groups were also injected with RAW 264.7 as the reporter macrophages. Wear particle-induced bone loss and the effects of 7ND were evaluated by microCT, immunohistochemical staining, and bioluminescence imaging. Local delivery of 7ND using the LBL coating decreased systemic macrophage recruitment, the number of osteoclasts and wear particle-induced bone loss. The development of a novel orthopaedic implant coating with anti-CCL2 protein may be a promising strategy to mitigate peri-prosthetic osteolysis.

Keywords

osteolysis; mutant CCL2 protein; implant coating; macrophage; total joint replacement

*Please address correspondence to: Stuart B. Goodman MD PhD, Department of Orthopaedic Surgery, Stanford University School of Medicine, 450 Broadway Street, Redwood City, CA, USA, 94063, Phone: 01-650-721-7662, FAX: 01-650-721-3470, goodbone@stanford.edu.

Introduction

Total joint replacement (TJR) is a highly successful and widely used surgical procedure for patients with end-stage degenerative and inflammatory arthritis. However the long-term survival of replacements is limited by wear of their load bearing surfaces [1–3]. Wear particles are inevitable byproducts of all TJR procedures; they stimulate chronic inflammation that delays osseointegration, leading to peri-prosthetic bone loss (osteolysis) and eventual loosening of the implant [4]. Currently, no clinically successful non-surgical treatments for wear particle-induced osteolysis exist. Revision surgical procedures are technically more difficult than primary procedures and carry high rates of complication. Therefore, new strategies are required for reducing wear particle-induced osteolysis to prolong the lifespan of TJRs.

Monocyte/macrophage lineage cells (macrophages, foreign body giant cells and osteoclasts) are the key players of chronic inflammation, the foreign body reaction to wear particles, and peri-prosthetic osteolysis [1, 5, 6]. In the peri-prosthetic tissues, macrophages are activated by wear particles to release pro-inflammatory cytokines and chemokines which induce systemic macrophage recruitment, thereby accelerating inflammation and subsequent bone resorption by osteoclasts [4, 5]. Monocyte Chemoattractant Protein-1 (MCP-1, also known as CCL2) is one of the main chemokines regulating systemic and local trafficking of monocyte/macrophages in particle-induced inflammation. Osteoblasts and fibroblasts in the peri-implant tissue also release CCL2 in the presence of wear particles, however macrophages, especially M1 (pro-inflammatory) macrophages, are the main source of CCL2 secretion [7, 8]. Retrieval studies have shown that the peri-implant tissue expresses high levels of CCL2 [9]. Furthermore, both wear particle-induced macrophage recruitment and bone loss were mitigated by inhibition of the interaction between CCL2 and its receptor CCR2 by systemic administration of a CCR2 antagonist in vivo [10]. 7ND recombinant protein is a mutant CCL2 protein, which lacks the amino acids 2 through 8 on the N-terminal, and acts as a dominant negative inhibitor of CCL2 [11–13]. Anti-CCL2 therapy has been successfully applied following drug-eluting coronary stents, which attenuated monocyte/macrophage infiltration and unwanted neointimal formation [14, 15]. A previous in vitro study suggested that 7ND may be used as an inhibitor to reduce wear particle-induced macrophage migration and cytokine release [16]. Moreover, 7ND locally injected onto the calvaria reduced wear particle-induced osteolysis in a murine calvarial osteolysis model [17]. We recently developed a layer-by-layer (LBL) platform for coating implant surfaces, which can accomplish controlled release of biologically active 7ND protein [18]. We hypothesized that 7ND locally released from LBL coated implants can mitigate wear particle-induced macrophage recruitment and subsequent bone loss. In this study, we investigated the effect of 7ND protein coating on wear particle-induced bone loss using the clinically relevant murine continuous femoral intramedullary polyethylene (PE) particle infusion model with 7ND coating of a titanium rod as a local drug delivery device.

Materials and Methods

7ND coated rod

Hollow A-40 titanium rods (6 mm, 21 G, New England Small Tube, Litchfield, NH) were coated with a 7ND-releasing coating following a LBL method previously established [18]. End-modified poly (β-amino ester) (C32-130) was synthesized as described [18], and used as the positively charged polyelectrolyte (10 mg/ml). Polystyrene sulfonate (3 mg/ml) was used as the negatively charged polyelectrolyte. 7ND was suspended in 0.1% bovine serum albumin at 30 μg/ml. To aid the attachment of the coating, titanium rods were surface etched with concentrated hydrochloric acid for 2 h. Rods were then washed with H_2O and ethanol. After air drying, LBL deposition was performed with polyelectrolyte layers on the bottom deposited for 5 min, and the 7ND layer on top deposited for 10 min. Rods were washed in H_2O between layer depositions. The sustained release of 7ND from the surface coating was confirmed in vitro using a CCL2 ELISA Kit (Peprotech, Rocky Hill, NJ) and bioactivity was confirmed by macrophage migration assay as previously described [18].

Isolation of polyethylene particles and osmotic pumps

Clinically relevant conventional ultrahigh molecular weight polyethylene (UHMWPE) particles were a kind gift from Dr. Timothy Wright, Hospital for Special Surgery, New York. Particles were obtained from joint simulator tests and isolated according to an established centrifugation protocol [19]. Frozen aliquots of particle-containing serum were lyophilized for 4–7 days. The dried material was digested in 5 M sodium hydroxide at 60 °C for 1 h, followed by ultrasonication for 10 min. The digested particle suspension was centrifuged through a 5% sucrose gradient at 40,000 rpm at 10 °C for 3 h. The collected particles at the surface of the sucrose solution were incubated at 80 °C for 1 h before ultrasonication, and centrifugation through an isopropanol gradient (0.96 and 0.90 g/cm^3) at 40,000 rpm at 10 °C for 1 h. The purified particles at the interface between the two layers of isopropanol were collected. Isopropanol was evaporated from the particle mixture which was then lyophilized. After lyophilization, the particles were suspended in phosphate buffered saline (PBS) and kept in a −80 °C freezer. The particles tested negative for endotoxin by a Limulus Amebocyte Lysate Kit (Lonza, Allendale, NJ). The mean diameter of the particles was 0.48±0.10 μm (mean ±standard error, averaged from 125 scanned particles) measured by electron microscopy. An Alzet mini osmotic pump model 2006 (Durect Corporation, Cupertino, CA) was loaded with PE particles (15 mg/ml) or PBS. The pumps and the titanium rods were connected via a 6 cm vinyl catheter tubing (Durect Corporation) which was prefilled with PE particle solution or PBS.

Mouse model of particle-induced osteolysis and experimental design

The murine continuous femoral intramedullary PE particle infusion model was performed as previously described.[20] Six experimental groups were established (Table 1): Group 1, PBS + control rod; Group 2, PBS + 7ND coated rod; Group 3, PE particles + control rod; Group 4, PE particles + 7ND coated rod; Group 5, PE particles + control rod + RAW 264.7 cell injection via the tail vein; Group 6, PE particles + 7ND coated rod + RAW 264.7 cell injection. For each group, twelve athymic nude male mice (Crl:NU(NCr)-*Foxn1*^{nu}, 11-12 weeks old, Charles River Laboratory Inc., Wilmington, MA) were used. The experimental

design was approved by the Institutional Administration Panel for Laboratory Animal Care at Stanford University. Under inhalation anesthesia, we approached the right distal femur via a lateral parapatellar incision, and pierced through the intercondylar notch to access the medullary cavity by a series of needles (25–21 gauge). The titanium rod with or without 7ND coating was press-fit into the distal femur. An osmotic pump containing PE particles or PBS was implanted into dorsal side of the mouse subcutaneously through a second incision and connected to the implanted rod via subcutaneous vinyl catheter tubing. Skin incisions (knee and dorsal) were closed with 5–0 Ethilon sutures. Buprenorphine (0.1 mg/kg s.c.) was used for postoperative analgesia.

MicroCT

MicroCT scans were performed immediately pre-operation and 4 weeks after operation for Group 1 to 4 using eXplore Locus RS150 microCT (GE Healthcare, Fairfield, CT) with 49 μm resolution. At the post-operation scanning, mice were euthanized and the titanium rod removed from the distal femur before microCT scan was performed. A phantom that mimics hydroxyapatite and contains water and air inclusions was used for image calibration. A 3D region of interest (ROI, 4 mm × 4 mm × 3 mm) was created which contained only the diaphysis proceeding proximally, beginning 3 mm from the distal end of the femur. The thresholded bone mineral density (BMD) was quantified and analyzed by using GEMS MicroView software (threshold: 700 HU). BMD was normalized by the value of pre-operation scan (postop – preop value).

Reporter cell and bioluminescence imaging

Murine reporter macrophages were injected into the tail vein to simulate the systemic trafficking of macrophages in the presence of an inflammatory stimulus, namely the local infusion of wear particles into the distal femur. The murine macrophage cell line RAW 264.7 transfected with the lentiviral vector to express the bioluminescent optical reporter gene, firefly luciferase (*fluc*), and a fluorescence reporter gene, green fluorescent protein (*gfp*) was used as a reporter cell for systemic macrophage recruitment to the area of inflammation [21]. The cells were cultured in Dulbecco's Modified Eagle Medium (DMEM) supplemented with 10% Fetal Bovine Serum (FBS) and an antibiotic/antimycotic solution (100 units of penicillin, 100 μg of streptomycin, and 0.25 μg of Amphotericin B per ml; Hyclone, Thermo Scientific). One week after operation for Groups 5 and 6, RAW 264.7 reporter cells (0.5×10^6 cells suspended in 0.1 ml Hank's Balanced Salt Solution, Invitrogen, Carlsbad, CA) were injected to the systemic circulation through a lateral tail vein. IVIS-100 (Perkin Elmer, Waltham, MA) was used for in vivo bioluminescence imaging (BLI). Luciferase substrate D-luciferin was administrated by intraperitoneal injection (3 mg/mouse). Ten minutes after substrate injection, lateral images were taken of the whole mouse. Mice were imaged immediately after macrophage injection (day 0), then imaged every other day for two weeks (day 14). Images were quantified by drawing a uniformly sized circular ROI (1.5 cm) to right distal femur and rectangular ROI for whole body adjusted with each mouse. The data were collected and expressed as photon/second/cm^2/steradian (p/s/cm^2/sr). After imaging at day 14, mice were euthanized and femora were collected.

Immunohistochemistry and cell counting

Femora were collected after post-operation microCT scanning for Group 1 to 4 or after BLI at day 14 for Group 5 and 6. The femora were fixed in 4% paraformaldehyde (PFA) for 3 days, and decalcified in 0.5 M ethylenediamine tetra acetic acid (EDTA) for 2 weeks, and then embedded in optimal cutting temperature compound (Scigen Scientific, Gardena, CA). The frozen specimens were cut into 10 μm transverse sections for histological and immunohistochemical staining.

Macrophages were identified by direct immunofluorescence staining with F4/80 antibody. After blocking with 5% goat serum in PBS, the samples were incubated with FITC-conjugated rat anti-F4/80 antibody (1:50, AbD Serotec, Raleigh, NC) for 2 h at room temperature. The slides were mounted with ProLong Gold Antifade Mount with DAPI (Life Technologies, Grand Island, NY), and imaged using Axio Observer 3.1 fluorescence microscope (Zeiss, Oberkochen, Germany). F4/80 positive cells were counted manually in three random fields of view. Osteoblasts were detected by Avidin-biotin complex immunohistochemistry with anti-alkaline phosphatase (ALP) antibody. Endogenous peroxidase blocking was performed with BLOXALL blocking solution (Vector Laboratories, Burlingame, CA) for 10 minutes. After blocking with 10% rabbit serum for 1h, the samples were incubated with goat anti-mouse ALP antibody (1:80, R&D, Minneapolis, MN) overnight at 4 °C. Biotinylated rabbit anti-goat antibody (1:200, Vector Laboratories) was used as a secondary antibody, followed by labeling with Vectastain Elite ABC kit (Vector Laboratories). The reaction products were visualized with Vector NovaRed Peroxide Substrate kit (Vector Laboratories) and counterstained with hematoxylin. ALP positive cells were manually counted and normalized by the total length of the endosteum quantified by ImageJ (NIH, Bethesda, MD). Osteoclast-like cells were determined using a leukocyte tartrate resistant acid phosphatase (TRAP) kit (Sigma Aldrich, St. Louis, MO) as multinucleated cells located on the bone perimeter within the resorption lacunae. The positively stained cells were counted manually and normalized by the bone area quantified by ImageJ software. RAW 264.7 reporter cells were identified by direct immunofluorescence staining with GFP antibody. After antigen retrieval with proteinase K (Dako, Glostrup, Denmark) for 3 minutes and blocking with 5% goat serum in PBS for 1h, the samples were incubated with Alexa Fluor 488-conjugated rabbit anti-GFP antibody (1:200, Invitrogen, Carlsbad, CA) overnight at 4 °C. GFP positive cells were counted manually in three random fields of view. The cell count was performed in a blind manner by two investigators.

Statistical analysis

Mice with placement of a misaligned rod or that sustained an intra-operative femur fracture were excluded from the analysis. The final sample size was 9 to 12 mice per group (Table 1). A one-way ANOVA with Tukey's post-hoc test was used for the results of microCT and immunostaining. The non-paired t-test was used for two-group comparisons. All data analysis was performed using Prism 6 (GraphPad Software, La Jolla, CA). $P < 0.05$ was considered as the threshold for statistical significance. Data is reported as mean ± standard error of the mean.

Results

7ND coating prevented PE-induced bone loss

To investigate the ability of 7ND coating to mitigate wear particle-induced bone loss in vivo, the BMD of the ROI in the distal femur was evaluated by microCT (Figure 1a, b). BMD of the PE + control rod group was significantly reduced compared to the value of PBS + control rod group ($p = 0.0016$). The 7ND coated group significantly prevented the PE-induced bone loss ($p = 0.0128$). Interestingly, the PBS + 7ND coated rod group decreased the BMD compared with PBS + control rod group, but the difference did not reach statistical significance ($p = 0.1173$).

7ND coating reduced the number of macrophages induced by PE particles

Sections from the particle infusion area were stained for macrophages using F4/80 antibody and examined with immunofluorescence (Figure 2). F4/80 positive cells in PE + control rod group were significantly increased compared to the control group ($p < 0.001$). The 7ND coated group demonstrated a significant reduction in the number of macrophages in the presence of PE particles ($p < 0.001$).

7ND coating reduced the number of osteoclasts induced by PE particles

The number of osteoclast-like cells was identified by TRAP staining (Figure 3a, b). TRAP positive cells were significantly increased in the PE + control rod group compared to the PBS + control rod ($p = 0.0339$). 7ND coating reversed the increase in TRAP positive cells induced by PE particles ($p = 0.0458$). The number of osteoblasts determined by ALP staining showed no significant differences among the four experimental groups (Figure 3a, c).

7ND mitigated the accumulation of reporter macrophages to the PE particle infusion site

The effect of 7ND coating on PE particle induced systemic macrophage recruitment was investigated by BLI following the injection of luciferase and GFP expressing RAW 264.7 reporter macrophages to systemic circulation (Figure 4a). From day 10 to day 14, the BLI signal ratio (operated femur / whole body) originating from the region of interest in the distal femur was significantly reduced in the 7ND coated rod group compared to the control rod group (Figure 4b, day 10, $p = 0.0390$; day 12, $p = 0.005$; day 14, $p = 0.015$). Corresponding results were obtained with immunostaining of the femur sections in which GFP positive cells infiltrating the femur infused with PE particles were also significantly decreased in the 7ND rod group (Figure 4c, d, $p < 0.001$).

Discussion

In the process of peri-prosthetic osteolysis, macrophages play a pivotal role. Macrophages activated by wear particles secrete pro-inflammatory cytokines, chemokines and other factors that lead to further macrophage recruitment, chronic inflammation, increased osteoclastogenesis and suppressed osteoblast formation and function [6]. As a result, these reactions change the local bone microenvironment from net bone formation to net bone

resorption, thus leading to peri-prosthetic osteolysis, jeopardizing the underlying bone supporting the prosthesis.

Wear particle-activated cells release pro-inflammatory cytokines and chemokines such as tumor necrosis factor-α (TNF-α), interleukin (IL)-1β, IL-6, IL-8, prostaglandin E2 (PGE2), CCL2 and CCL3 [22]. Thus, the strategy to potentially mitigate inflammation induced by wear particles by interruption of the continuous recruitment of monocyte/macrophages from the circulation to the implant site by inhibiting the chemokine-receptor axis is an innovative therapeutic approach. The chemokine CCL2 is a member of the C-C chemokine family, and is an immediate early stress responsive factor [23]. Both CCL2 and its receptor CCR2 have been demonstrated to play important roles in inflammatory diseases [23–26], CCL2 regulates the migration and infiltration of pro-inflammatory cells (monocytes/macrophages, neutrophils and, lymphocytes); thus CCL2-CCR2 ligand-receptor axis is a potential target for treatment of chronic inflammation [14, 26–28]. In regard to peri-prosthetic osteolysis, previous in vitro studies have shown that macrophages challenged with polyethylene, polymethylmethacrylate,, and titanium-alloy particles released high amounts of CCL2 [29, 30]. In addition, the peri-implant tissues derived from osteolytic lesion of human clinical samples expressed high levels of CCL2 [9]. Our previous in vivo study has shown that injection of CCR2 antagonist inhibited PE particle-induced systemic migration of macrophages and prevented the suppression of bone mineral density due to PE particles [10]. These results suggested the CCL2-CCR2 ligand-receptor axis is strongly involved in particle-induced peri-prosthetic osteolysis. Furthermore, local injection of 7ND protein reduced wear particle-induced osteolysis in vivo using the mouse calvarial model with local injection of 7ND protein [17]. However this model involves a single bolus administration of PE particles onto a flat bone, which does not simulate the clinical scenario of continuous wear particle delivery into a long bone. In the current study, we inhibited CCL2-CCR2 axis by 7ND protein locally delivered using the LBL coating method in an in vivo murine continuous particle infusion model. The advantages of the current study are both the use of controlled-release local delivery system of anti-CCL2 molecules and the assessment in an in vivo model using the mouse femur, which better mimics continuous particle production seen in human joint replacements.

Local drug delivery systems have several advantages compared to systemic treatments. These advantages include targeted anatomic delivery of biologics to the local site, lower dosage requirement, and reduction of potentially serious systemic side effects. Among orthopaedic devices, coating of implants with biomolecules is one method of local delivery [31]. To achieve the desirable effect, it is critical to develop methods to enable efficient loading of biomolecules onto the implant surface as well as modulate the controlled release while retaining their specific biological functions. The layer-by-layer coating platform is a promising technique for local drug delivery [32, 33]. Several studies demonstrated new implant coating strategies using LBL coating targeting infection and bone formation [34, 35], but few studies have used this method to mitigate peri-prosthetic inflammation and osteolysis directly. We have recently developed a layer-by-layer coating platform on implant surfaces that demonstrates controlled release of 7ND protein with retained biological activity in vitro [18]. Our results demonstrated 7ND coating using the LBL platform significantly decreased wear particle-induced bone loss in vivo. These results suggest that

anti-CCL2 protein coating by LBL platform is a promising strategy to mitigate peri-prosthetic osteolysis.

Using a multi-scale assessment, we confirmed that the 7ND coating reduced the number of infiltrated macrophages and osteoclasts, while the number of osteoblasts remained stable. These results suggest that 7ND acts as an anti-resorptive mechanism rather than enhancing new bone formation directly. In addition, our previous study showed that 7ND protein prevents not only particle-induced macrophage chemotaxis, but also particle-induced inflammation in vitro [16]. Furthermore, 7ND has been shown to inhibit osteoclast differentiation of human colony forming unit-granulocyte macrophages (CFU-GM) in vitro [36]. Taken together 7ND coating reduced both the number of infiltrating macrophages and possibly the amount of particle-induced secretion of pro-inflammatory factors. 7ND might also directly inhibit osteoclast differentiation, thus mitigating cell recruitment, local inflammation and also directly, osteoclastogenesis.

During the normal bone fracture healing process, monocytes/macrophages are thought to play a pivotal role in the regulation of bone metabolism through stimulating bone resorption or bone formation [37]. CCL2 is also thought to be a mediator of bone remodeling by recruiting monocytes/macrophages to the site of bone injury [38]. A recent study showed that CCL2-CCR2 signaling during the early phase of fracture healing is crucial for recruitment of mesenchymal progenitor cells [39]. Our results showed 7ND coating without PE particle infusion tended to decrease BMD compared to controls, while 7ND reversed PE particle-induced bone loss in PE particle infused group. These results suggest that 7ND has not only an effect on mitigation of bone loss induced by excessive inflammatory stimuli, but may alter homeostatic bone remodeling. Further investigation is required to determine the optimal conditions for clinical applications.

To interrupt the CCL2-CCR2 axis, several types of inhibitors such as CCR2 antagonist, neutralizing antibody of CCL2, CCL2 mutant protein with property of inhibiting CCL2 singling and RNA interference technology have been investigated for treatment of cardiovascular disease, neurodegenerative disease, cancer, and chronic inflammatory diseases [24, 40–44]. Our previous studies [16–18] and the current study demonstrate the positive effects of 7ND, a dominant negative mutant CCL2, on mitigating wear particle-induced bone loss. Further studies are needed to elucidate the effective combinations of molecules and drug delivery systems to mitigate peri-prosthetic osteolysis.

Several limitations in the present study should be noted. First, the current protocol was not designed to test all strategies by which 7ND interferes with CCL2-CCR2 signaling. Further studies using CCL2 knockout mice and/or CCR2 depleted reporter macrophages would prove useful to further examine the direct effects of 7ND on interrupting the CCL2-CCR2 signaling axis. Second the experiments were conducted using nude mice, a type of immune-compromised mice, to allow the use of exogenous reporter macrophages to quantify the cell recruitment to the peri-implant tissues. It can be questioned how closely the inflammatory response to wear particles in this model system resembles that the clinical scenario that develops in subjects with an intact immune system. Indeed, scattered T cells are present in the retrieved tissues surrounding loosening implants [45, 46], but it also has been shown that

T cells are not required for the development of particle induced inflammation and osteolysis nor the foreign body reaction in mouse models [47, 48]. Furthermore we recently showed in the mouse calvarial model that local 7ND injections mitigated wear particle induced osteolysis in wild type mice with an uncompromised (normal) immune system [17]. Nevertheless it would be important to demonstrate the effect of 7ND coated implant on wear particle-induced osteolysis in an immunocompetent model.

Third, we used RAW 264.7 cells as the reporter cells to quantitate the systemic recruitment of circulating macrophages to the area of particle induced inflammation. RAW 264.7 cells are an immortal macrophage cell line established from leukemia and thus these cells have an ability to migrate systemically, in bone marrow in particular, and proliferate at the local site. Thus the BLI signal reflects not only systemic trafficking, but also the local proliferative capacity of RAW cells. In addition, RAW cells may cause cachexia of the mice 2 to 3 weeks after cell injection due to excessive proliferation. To prevent early onset of cachexia, the amount of RAW cells injected to the systemic circulation was relatively small. Due to the threshold of sensitivity of the IVIS system, this small number of cells initially migrating to the area of inflammation showed inadequate signal to detect the difference between the control rod and 7ND coated rod groups in the first week of the systemic reporter cell injection; as the cells proliferated locally and more cells were recruited, the difference between the groups became apparent in the second week of BLI. Furthermore since inflammatory macrophages are the primary source of CCL2 secretion, the difference between 7ND and control groups was probably further amplified and thus easier to detect at a later time point. Based on these facts, primary macrophage with the GFP/FLUC reporter gene is an appropriate reporter cell to evaluate the systemic trafficking of macrophages [49]. Indeed, we have shown previously that murine primary macrophages injected to the systemic circulation home to the area of particle-induced inflammation similar to RAW cells used in the current study [10, 49]

Conclusions

Local delivery of 7ND anti-CCL2 protein using the LBL coating technique mitigated PE wear particle-induced bone loss in a murine continuous polyethylene particle infusion model. The possible underlying mechanism is that 7ND decreased the systemic recruitment of monocyte/macrophage/osteoclast lineage, inhibiting both the macrophage-driven inflammation and subsequent osteoclastic-bone resorption. The development of a novel orthopaedic implant coating with anti-CCL2 protein may be a promising strategy to mitigate peri-prosthetic osteolysis and potentially extend the lifetime of TJRs.

Acknowledgement

This work was supported by NIH grants 2R01AR055650, 1R01AR063717, and the Ellenburg Chair in Surgery at Stanford University.

References

[1]. Gallo J, Goodman SB, Konttinen YT, Raska M. Particle disease: biologic mechanisms of periprosthetic osteolysis in total hip arthroplasty. Innate Immun. 2013; 19(2):213–24. [PubMed: 22751380]

[2]. Purdue PE, Koulouvaris P, Nestor BJ, Sculco TP. The central role of wear debris in periprosthetic osteolysis. Hss j. 2006; 2(2):102–13. [PubMed: 18751821]

[3]. Marshall A, Ries MD, Paprosky W. How prevalent are implant wear and osteolysis, and how has the scope of osteolysis changed since 2000? J Am Acad Orthop Surg. 2008; 16(Suppl 1):S1–6.

[4]. Goodman SB, Gibon E, Yao Z. The basic science of periprosthetic osteolysis. Instr Course Lect. 2013; 62:201–6. [PubMed: 23395025]

[5]. Nich C, Takakubo Y, Pajarinen J, Ainola M, Salem A, Sillat T, Rao AJ, Raska M, Tamaki Y, Takagi M, Konttinen YT, Goodman SB, Gallo J. Macrophages-Key cells in the response to wear debris from joint replacements. J Biomed Mater Res A. 2013; 101(10):3033–45. [PubMed: 23568608]

[6]. Ingham E, Fisher J. The role of macrophages in osteolysis of total joint replacement. Biomaterials. 2005; 26(11):1271–86. [PubMed: 15475057]

[7]. Pajarinen J, Kouri VP, Jamsen E, Li TF, Mandelin J, Konttinen YT. The response of macrophages to titanium particles is determined by macrophage polarization. Acta Biomater. 2013; 9(11): 9229–40. [PubMed: 23827094]

[8]. Tuan RS, Lee FY, Y TK, Wilkinson JM, Smith RL. What are the local and systemic biologic reactions and mediators to wear debris, and what host factors determine or modulate the biologic response to wear particles? J Am Acad Orthop Surg. 2008; 16(Suppl 1):S42–8. [PubMed: 18612013]

[9]. Jamsen E, Kouri VP, Olkkonen J, Cor A, Goodman SB, Konttinen YT, Pajarinen J. Characterization of macrophage polarizing cytokines in the aseptic loosening of total hip replacements. J Orthop Res. 2014; 32(9):1241–6. [PubMed: 24897980]

[10]. Gibon E, Ma T, Ren PG, Fritton K, Biswal S, Yao Z, Smith L, Goodman SB. Selective inhibition of the MCP-1-CCR2 ligand-receptor axis decreases systemic trafficking of macrophages in the presence of UHMWPE particles. J Orthop Res. 2012; 30(4):547–53. [PubMed: 21913218]

[11]. Zhang YJ, Rutledge BJ, Rollins BJ. Structure/activity analysis of human monocyte chemoattractant protein-1 (MCP-1) by mutagenesis. Identification of a mutated protein that inhibits MCP-1-mediated monocyte chemotaxis. J Biol Chem. 1994; 269(22):15918–24. [PubMed: 8195247]

[12]. Zhang Y, Rollins BJ. A dominant negative inhibitor indicates that monocyte chemoattractant protein 1 functions as a dimer. Mol Cell Biol. 1995; 15(9):4851–5. [PubMed: 7651403]

[13]. Ni W, Egashira K, Kitamoto S, Kataoka C, Koyanagi M, Inoue S, Imaizumi K, Akiyama C, Nishida KI, Takeshita A. New anti-monocyte chemoattractant protein-1 gene therapy attenuates atherosclerosis in apolipoprotein E-knockout mice. Circulation. 2001; 103(16):2096–101. [PubMed: 11319201]

[14]. Egashira K, Nakano K, Ohtani K, Funakoshi K, Zhao G, Ihara Y, Koga J, Kimura S, Tominaga R, Sunagawa K. Local delivery of anti-monocyte chemoattractant protein-1 by gene-eluting stents attenuates in-stent stenosis in rabbits and monkeys. Arterioscler Thromb Vasc Biol. 2007; 27(12): 2563–8. [PubMed: 17885211]

[15]. Ohtani K, Usui M, Nakano K, Kohjimoto Y, Kitajima S, Hirouchi Y, Li XH, Kitamoto S, Takeshita A, Egashira K. Antimonocyte chemoattractant protein-1 gene therapy reduces experimental in-stent restenosis in hypercholesterolemic rabbits and monkeys. Gene Ther. 2004; 11(16):1273–82. [PubMed: 15175640]

[16]. Yao Z, Keeney M, Lin TH, Pajarinen J, Barcay K, Waters H, Egashira K, Yang F, Goodman S. Mutant monocyte chemoattractant protein 1 protein attenuates migration of and inflammatory cytokine release by macrophages exposed to orthopedic implant wear particles. J Biomed Mater Res A. 2014; 102(9):3291–7. [PubMed: 24123855]

[17]. Jiang X, Sato T, Yao Z, Keeney M, Pajarinen J, Lin TH, Loi F, Egashira K, Goodman S, Yang F. Local delivery of mutant CCL2 protein reduced orthopaedic implant wear particle-induced osteolysis and inflammation in vivo. J Orthop Res. 2015

[18]. Keeney M, Waters H, Barcay K, Jiang X, Yao Z, Pajarinen J, Egashira K, Goodman SB, Yang F. Mutant MCP-1 protein delivery from layer-by-layer coatings on orthopedic implants to modulate inflammatory response. Biomaterials. 2013; 34(38):10287–95. [PubMed: 24075408]

[19]. Campbell P, Ma S, Yeom B, McKellop H, Schmalzried TP, Amstutz HC. Isolation of predominantly submicron-sized UHMWPE wear particles from periprosthetic tissues. J Biomed Mater Res. 1995; 29(1):127–31. [PubMed: 7713952]

[20]. Ma T, Huang Z, Ren PG, McCally R, Lindsey D, Smith RL, Goodman SB. An in vivo murine model of continuous intramedullary infusion of polyethylene particles. Biomaterials. 2008; 29(27):3738–42. [PubMed: 18561997]

[21]. De A, Lewis XZ, Gambhir SS. Noninvasive imaging of lentiviral-mediated reporter gene expression in living mice. Mol Ther. 2003; 7(5 Pt 1):681–91. [PubMed: 12718911]

[22]. Pajarinen J, Lin TH, Sato T, Yao Z, Goodman S. Interaction of Materials and Biology in Total Joint Replacement - Successes, Challenges and Future Directions. J Mater Chem B Mater Biol Med. 2014; 2(41):7094–7108. [PubMed: 25541591]

[23]. Deshmane SL, Kremlev S, Amini S, Sawaya BE. Monocyte chemoattractant protein-1 (MCP-1): an overview. J Interferon Cytokine Res. 2009; 29(6):313–26. [PubMed: 19441883]

[24]. Bose S, Cho J. Role of chemokine CCL2 and its receptor CCR2 in neurodegenerative diseases. Arch Pharm Res. 2013; 36(9):1039–50. [PubMed: 23771498]

[25]. Lee HW, Choi HJ, Ha SJ, Lee KT, Kwon YG. Recruitment of monocytes/macrophages in different tumor microenvironments. Biochim Biophys Acta. 2013; 1835(2):170–9. [PubMed: 23287570]

[26]. Panee J. Monocyte Chemoattractant Protein 1 (MCP-1) in obesity and diabetes. Cytokine. 2012; 60(1):1–12. [PubMed: 22766373]

[27]. Baay M, Brouwer A, Pauwels P, Peeters M, Lardon F. Tumor cells and tumor-associated macrophages: secreted proteins as potential targets for therapy. Clin Dev Immunol. 2011; 2011:565187. [PubMed: 22162712]

[28]. Zhang J, Patel L, Pienta KJ. Targeting chemokine (C-C motif) ligand 2 (CCL2) as an example of translation of cancer molecular biology to the clinic. Prog Mol Biol Transl Sci. 2010; 95:31–53. [PubMed: 21075328]

[29]. Huang Z, Ma T, Ren PG, Smith RL, Goodman SB. Effects of orthopedic polymer particles on chemotaxis of macrophages and mesenchymal stem cells. J Biomed Mater Res A. 2010; 94(4): 1264–9. [PubMed: 20694994]

[30]. Nakashima Y, Sun DH, Trindade MC, Chun LE, Song Y, Goodman SB, Schurman DJ, Maloney WJ, Smith RL. Induction of macrophage C-C chemokine expression by titanium alloy and bone cement particles. J Bone Joint Surg Br. 1999; 81(1):155–62. [PubMed: 10068024]

[31]. Goodman SB, Yao Z, Keeney M, Yang F. The future of biologic coatings for orthopaedic implants. Biomaterials. 2013; 34(13):3174–83. [PubMed: 23391496]

[32]. Zelikin AN. Drug releasing polymer thin films: new era of surface-mediated drug delivery. ACS Nano. 2010; 4(5):2494–509. [PubMed: 20423067]

[33]. Boudou T, Crouzier T, Ren K, Blin G, Picart C. Multiple functionalities of polyelectrolyte multilayer films: new biomedical applications. Adv Mater. 2010; 22(4):441–67. [PubMed: 20217734]

[34]. Perez-Anes A, Gargouri M, Laure W, Van Den Berghe H, Courcot E, Sobocinski J, Tabary N, Chai F, Blach JF, Addad A, Woisel P, Douroumis D, Martel B, Blanchemain N, Lyskawa J. Bioinspired Titanium Drug Eluting Platforms Based on a Poly-beta-cyclodextrin-Chitosan Layer-by-Layer Self-Assembly Targeting Infections. ACS Appl Mater Interfaces. 2015; 7(23):12882–93. [PubMed: 25992843]

[35]. Min J, Choi KY, Dreaden EC, Padera RF, Braatz RD, Spector M, Hammond PT. Designer Dual Therapy Nanolayered Implant Coatings Eradicate Biofilms and Accelerate Bone Tissue Repair. ACS Nano. 2016; 10(4):4441–50. [PubMed: 26923427]

[36]. Morrison NA, Day CJ, Nicholson GC. Dominant negative MCP-1 blocks human osteoclast differentiation. J Cell Biochem. 2014; 115(2):303–12. [PubMed: 23996571]

[37]. Xing Z, Lu C, Hu D, Yu YY, Wang X, Colnot C, Nakamura M, Wu Y, Miclau T, Marcucio RS. Multiple roles for CCR2 during fracture healing. Dis Model Mech. 2010; 3(7–8):451–8. [PubMed: 20354109]

[38]. Yadav A, Saini V, Arora S. MCP-1: chemoattractant with a role beyond immunity: a review. Clin Chim Acta. 2010; 411(21–22):1570–9. [PubMed: 20633546]

[39]. Ishikawa M, Ito H, Kitaori T, Murata K, Shibuya H, Furu M, Yoshitomi H, Fujii T, Yamamoto K, Matsuda S. MCP/CCR2 signaling is essential for recruitment of mesenchymal progenitor cells during the early phase of fracture healing. PLoS One. 2014; 9(8):e104954. [PubMed: 25133509]

[40]. Berman JP, Farkouh ME, Rosenson RS. Emerging anti-inflammatory drugs for atherosclerosis. Expert Opin Emerg Drugs. 2013; 18(2):193–205. [PubMed: 23675745]

[41]. Yumimoto K, Akiyoshi S, Ueo H, Sagara Y, Onoyama I, Ueo H, Ohno S, Mori M, Mimori K, Nakayama KI. F-box protein FBXW7 inhibits cancer metastasis in a non-cell-autonomous manner. J Clin Invest. 2015; 125(2):621–35. [PubMed: 25555218]

[42]. Semple BD, Kossmann T, Morganti-Kossmann MC. Role of chemokines in CNS health and pathology: a focus on the CCL2/CCR2 and CXCL8/CXCR2 networks. J Cereb Blood Flow Metab. 2010; 30(3):459–73. [PubMed: 19904283]

[43]. Gschwandtner M, Piccinini AM, Gerlza T, Adage T, Kungl AJ. Interfering with the CCL2-glycosaminoglycan axis as a potential approach to modulate neuroinflammation. Neurosci Lett. 2016; 626:164–73. [PubMed: 27212623]

[44]. Okamoto M, Fuchigami M, Suzuki T, Watanabe N. A novel C-C chemokine receptor 2 antagonist prevents progression of albuminuria and atherosclerosis in mouse models. Biol Pharm Bull. 2012; 35(11):2069–74. [PubMed: 23123476]

[45]. Goodman SB. Wear particles, periprosthetic osteolysis and the immune system. Biomaterials. 2007; 28(34):5044–8. [PubMed: 17645943]

[46]. Pajarinen J, Cenni E, Savarino L, Gomez-Barrena E, Tamaki Y, Takagi M, Salo J, Konttinen YT. Profile of toll-like receptor-positive cells in septic and aseptic loosening of total hip arthroplasty implants. J Biomed Mater Res A. 2010; 94(1):84–92. [PubMed: 20127718]

[47]. Taki N, Tatro JM, Nalepka JL, Togawa D, Goldberg VM, Rimnac CM, Greenfield EM. Polyethylene and titanium particles induce osteolysis by similar, lymphocyte-independent, mechanisms. J Orthop Res. 2005; 23(2):376–83. [PubMed: 15734251]

[48]. Rodriguez A, Macewan SR, Meyerson H, Kirk JT, Anderson JM. The foreign body reaction in T-cell-deficient mice. J Biomed Mater Res A. 2009; 90(1):106–13. [PubMed: 18491378]

[49]. Pajarinen J, Lin TH, Sato T, Loi F, Yao Z, Konttinen YT, Goodman SB. Establishment of Green Fluorescent Protein and Firefly Luciferase Expressing Mouse Primary Macrophages for In Vivo Bioluminescence Imaging. PLoS One. 2015; 10(11):e0142736. [PubMed: 26555613]

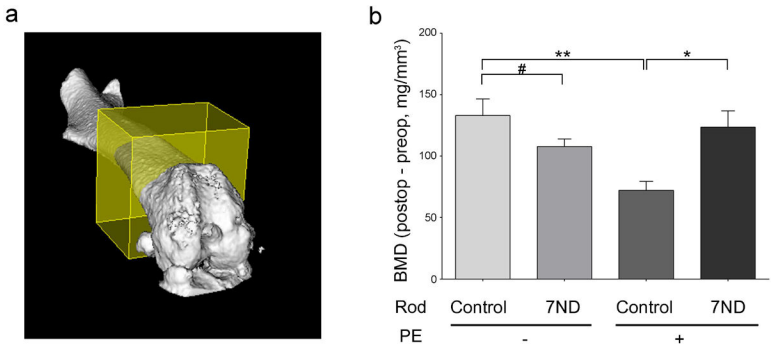

Figure 1. 7ND coating decreased PE wear particle-induced bone loss

MicroCT was performed pre-operatively and four weeks post-operatively. (**a**) 3D reconstruction image of the right femur after operation. The 3D region of interest (yellow cube) was defined as a 4 mm × 4 mm × 3 mm cube beginning 3 mm from the distal end of the femur. (**b**) Normalized bone mineral density (post-operation − pre-operation) was quantified in the indicated four groups (PBS + control rod, PBS + 7ND coated rod, PE + control rod, and PE + 7ND coated rod, n = 9). A one-way ANOVA with Tukey's post hoc test was used for statistical analysis. PE: UHMWPE particles. *$p < 0.05$, **$p < 0.01$, # not significant.

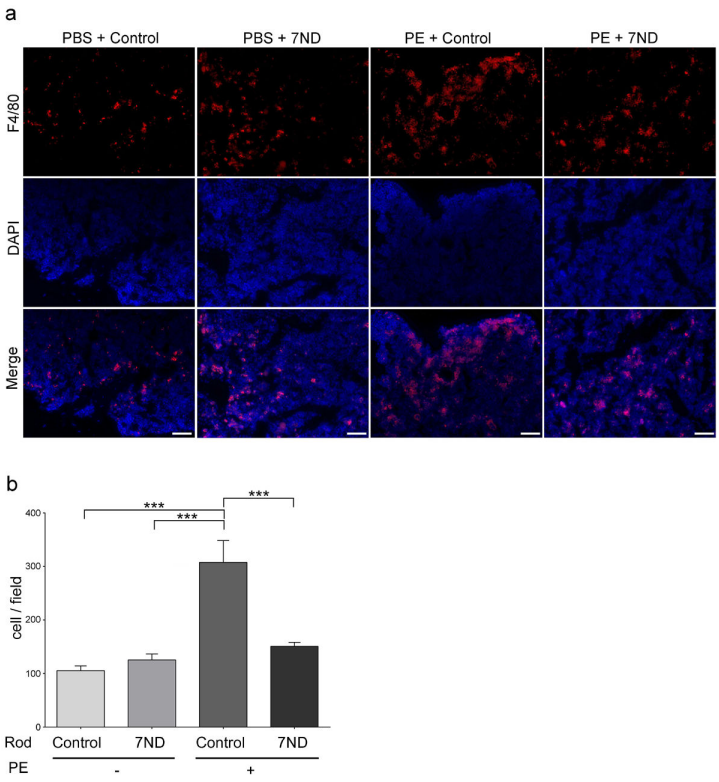

Figure 2. 7ND coating reduced PE wear particle –induced macrophage infiltration into distal femur

(**a**) Immunostaining of macrophages with FITC conjugated anti-F4/80 antibody (red). Nuclei were visualized with DAPI (blue). Scale bar: 50μm. (**b**) The number of F4/80 positive cells was counted in three randomly selected views (n = 4). A one-way ANOVA with Tukey's post hoc test was used for statistical analysis. PE: UHMWPE particles. ***$p < 0.001$.

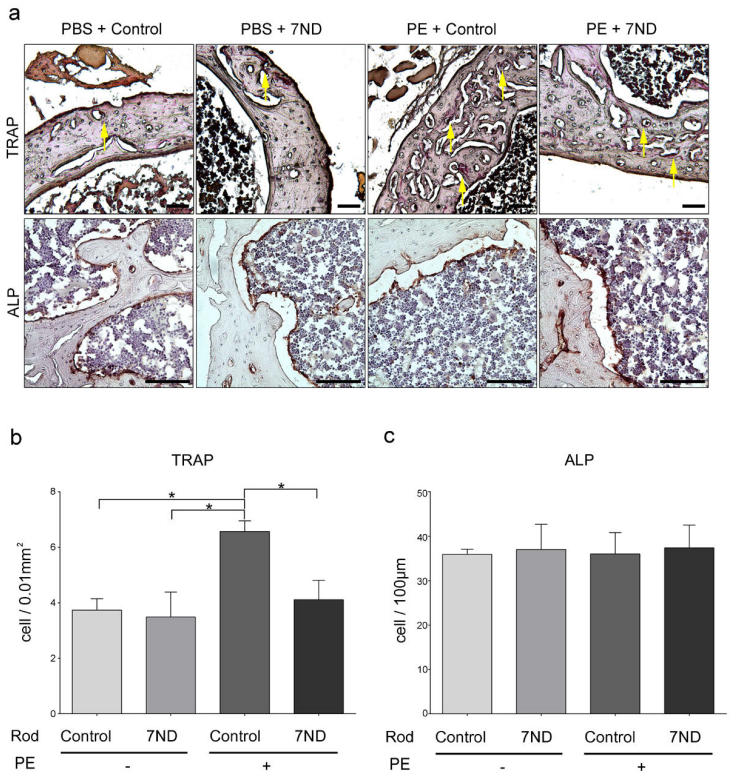

Figure 3. 7ND coating decreased the PE wear particle –induced increase in the number of osteoclasts in the distal femur, but had no significant effect on the number of osteoblasts

(**a**, upper) Osteoclasts were stained by leukocyte tartrate resistant acid phosphatase (TRAP). (a, lower) Alkaline phosphatase (ALP) antibody was used to identify osteoblasts. Yellow arrow shows TRAP positive cell. Scale bar: 50μm. (**b**) TRAP positive and (**c**) ALP positive cell numbers were counted, and the numbers were normalized by the bone area or total length of the endosteum, respectively (n = 4). A one-way ANOVA with Tukey's post hoc test was used for statistical analysis. *$p < 0.05$.

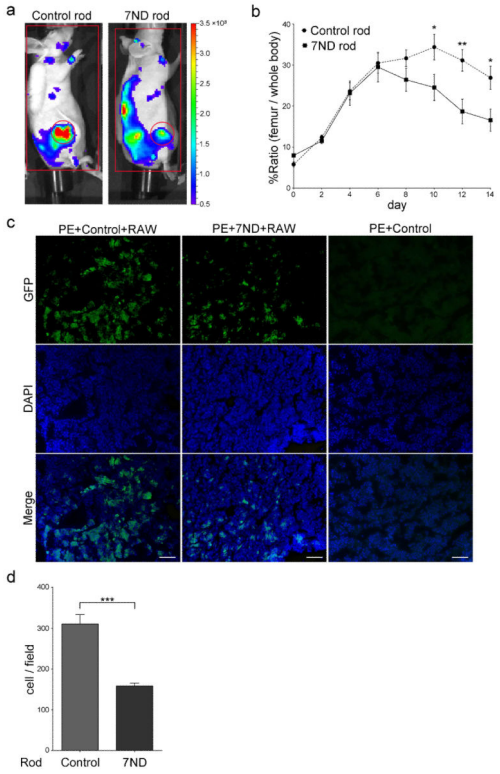

Figure 4. 7ND coating mitigated PE wear particle-induced systemic macrophage recruitment toward particle infused area

(**a**) Representative lateral images of bioluminescence imaging (BLI) of PE + control rod group and PE + 7ND rod group 14 days after RAW 264.7 reporter cell injection. Red circles indicate the region of interest defined for the distal femur, and red rectangles for the whole body. (**b**) The ratio (distal femur divided by whole body) of BLI was assessed until day 14 after cell injection. The non-paired t-test was used for statistical analysis (n = 11-12). (**c**) RAW 264.7 reporter cells were identified by immunostaining with Alexa Fluor 488 conjugated anti-GFP antibody. PE + control rod group (without RAW cell injection) was shown as negative control. Scale bar: 50μm. (**d**) The number of GFP positive cells in the bone marrow of the distal femur was counted in three randomly selected views (n = 4). The non-paired t-test was used for statistical analysis. PE: UHMWPE particles, RAW: RAW 264.7 cell. *p < 0.05, **p < 0.01, ***p < 0.001.

Table 1

Experimental Design of Murine Model

Group (n)	1 (9)	2 (9)	3 (9)	4 (9)	5 (11)	6 (12)
Rod	Control	7ND	Control	7ND	Control	7ND
PE particle			✓	✓	✓	✓
RAW cell					✓	✓

7ND, 7ND protein coating; PE, polyethylene; RAW cell, tail vein injection of RAW264.7 cells which expressed Green Fluorescent Protein and firefly luciferase as a reporter cell.